The Substrate Activation Process in the Catalytic Reaction of *Escherichia coli* Aromatic Amino Acid Aminotransferase†

Mohammad Mainul Islam, Hideyuki Hayashi, Hiroyuki Mizuguchi, and Hiroyuki Kagamiyama*

Department of Biochemistry, Osaka Medical College, 2-7 Daigakumachi, Takatsuki, Osaka 569-8686, Japan

Received June 27, 2000; Revised Manuscript Received September 7, 2000

ABSTRACT: Aromatic amino acid aminotransferase is active toward both aromatic and dicarboxylic amino acids, and the mechanism for this dual substrate recognition has been an issue in the enzymology of this enzyme. Here we show that, in the reactions with aromatic and dicarboxylic ligands, the pK_a of the Schiff base formed between the coenzyme pyridoxal 5′-phosphate and Lys258 or the substrate increases successively from 6.6 in the unliganded enzyme to ∼8.8 in the Michaelis complex and to >10.5 in the external Schiff base complex. Mutations of Arg292 and Arg386 to Leu, which mimic neutralization of the positive charges of the two arginine residues by the ligand carboxylate groups, increased the Schiff base pK_a by 0.1 and 0.7 unit, respectively. In contrast to these moderate effects of the Arg mutations, the cleavage of the Lys258 side chain of the Schiff base, which was brought about by preparing a mutant enzyme in which Lys258 was changed to Ala and the Schiff base was reconstituted with methylamine, produced the Schiff base pK_a value of 10.2, that being 3.6 units higher than that of the wild-type enzyme. The observation indicates that the Schiff base pK_a in the enzyme is lowered by the torsion around the C4−C4′ axis of the Schiff base and suggests that the pK_a is mainly controlled by changing the torsion angle during the course of catalysis. This mechanism, first observed for the reaction of aspartate aminotransferase with aspartate [Hayashi, H., Mizuguchi, H., and Kagamiyama, H. (1998) *Biochemistry 37*, 15076−15085], does not require the electrostatic contribution from the ω-carboxylate group of the substrate, and can explain why in aromatic amino acid aminotransferase the aromatic substrates can increase the Schiff base pK_a during catalysis to the same extent as the dicarboxylic substrates. This is the first example in which the torsion pK_a coupling of the pyridoxal 5′-phosphate Schiff base has been demonstrated in pyridoxal enzymes other than aspartate aminotransferase, and suggests the generality of the mechanism in the catalysis of aminotransferases related to aspartate aminotransferase.

Escherichia coli aromatic amino acid aminotransferase (ArAT,[1] aromatic amino acid:2-oxoglutarate aminotransferase, EC 2.6.1.57, also known as tyrosine aminotransferase) is a pyridoxal 5′-phosphate (PLP)-dependent enzyme and shows reversible transamination activities toward phenylalanine, tyrosine, tryptophan, aspartate, glutamate, and the corresponding keto acids, being able to recognize two structurally different sets of substrates, i.e., aromatic substrates and dicarboxylic substrates (*1*). ArAT shares many spectroscopic and kinetic properties with aspartate aminotransferase (AspAT) (*1*, *2*). The organization of the active site is essentially similar between the two enzymes (*3*, *4*; Figure 1). These findings strongly suggest that similar mechanisms work for the catalytic reactions of the two enzymes, especially for the reaction of aspartate and glutamate (and corresponding keto acids), which are the substrates common to the two enzymes.

For the reaction mechanism of AspAT with aspartate, there is a historically accepted mechanism in which the internal Schiff base (aldimine) formed between the ϵ-amino group of Lys258 and the coenzyme pyridoxal 5′-phosphate (PLP) acts as the acceptor for the proton of the ammonium (protonated amino) group of the substrate, thereby increasing the electrophilicity of the internal Schiff base and activating the substrate amino group for the nucleophilic attack on the Schiff base (*5*). This leads to a transaldimination reaction to form the Schiff base between the substrate and PLP (external Schiff base). The basis for this elegant "substrate-internal Schiff base co-activating" mechanism is the strikingly low basicity of the internal Schiff base in the unliganded enzyme. The pK_a ∼ 6.5, compared to the values of ∼10−11 of model Schiff bases in aqueous solutions (*6*). To explain this low pK_a value, Karpeisky and Ivanov (*7*) proposed that the two positive charges that are the anchoring sites for the substrate

† This work was supported by the "Research for the Future" Program (Project JSPS-RFTF96L00506 to H.K.), a Grant-in-Aid for Scientific Research (00183913 to H.H.) from the Japan Society for the Promotion of Science, and the SUNBOR Grant (to H.H.) from the Suntory Institute for Bioorganic Research.

* To whom correspondence should be addressed. Phone: +81-726-83-1221. Fax: +81-726-84-6516. E-mail: med001@art.osaka-med.ac.jp.

[1] Abbreviations: ArAT, aromatic amino acid aminotransferase (aromatic amino acid:2-oxoglutarate aminotransferase, EC 2.6.1.57); AspAT, aspartate aminotransferase (aspartate:2-oxoglutarate aminotransferase, EC 2.6.1.1); CD, circular dichroism; E_L, PLP form of the enzyme with an unprotonated Schiff base; E_LH^+, PLP form of the enzyme with a protonated Schiff base; E_M, PMP form of the enzyme; PLP, pyridoxal 5′-phosphate; PMP, pyridoxamine 5′-phosphate; HEPES, 1-(2-hydroxyethyl)piperazine-4-(2-ethanesulfonic acid); PIPES, 1,4-piperazinebis(ethanesulfonic acid); S, amino acid substrate (analogue) with an unprotonated α-amino group; SH^+, amino acid substrate (analogue) with a protonated α-amino group; TAPS, 3-{[(tris(hydroxymethyl)methyl]amino}-1-propanesulfonic acid.

10.1021/bi0014709 CCC: $19.00
Published on Web 11/23/2000

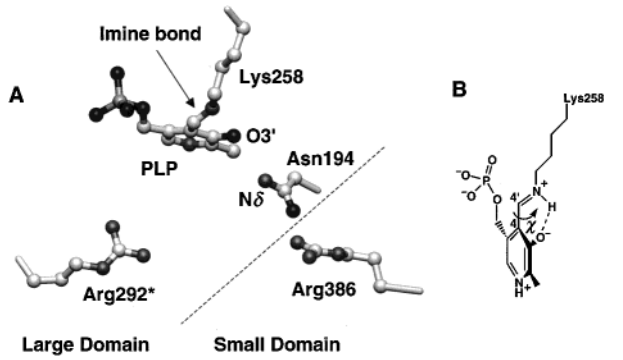

FIGURE 1: (A) Organization of the active site of ArAT. The crystal structure of pig cytosolic AspAT (1AJR; *4*) was used as the model. A hydrogen-bond linkage system is formed between O3′ of PLP, Asn194 (amide), and Arg386 (guanidinium). The substrate ω-carboxylate group of a dicarboxylic ligand forms a salt bridge or hydrogen bond with Arg292* and neutralizes its positive charge. A similar interaction is found between the substrate α-carboxylate group and Arg386. Additionally, the α-carboxylate group forms a hydrogen bond with Nδ of Asn194, resulting in the formation of a hydrogen-bond network involving the substrate−Arg386−Asn194−PLP complex. Among the residues shown here, only Arg386 belongs to the small domain. The dashed line shows the domain interface. (B) Schematic representation of the strain of the protonated Schiff base. With rotation around the C4−C4′ axis, the imine goes out of the plane of the pyridine ring, and the strain of the protonated Schiff base is increased. χ denotes the torsion angle around the C4−C4′ axis. This has a value of 0° when the imine is in the plane of the pyridine ring. In the structure of panel A, $\chi = 40°$.

carboxylate groups, later identified as Arg292* (for ω-carboxylate) and Arg386 (for α-carboxylate) by chemical modification (*8*) and X-ray crystallography (*9*, *10*), cause electrostatic repulsion with the protonated internal Schiff base. The binding of a dicarboxylic substrate neutralizes the positive charges and increases the internal Schiff base pK_a, thereby promoting the transfer of the proton from the substrate ammonium group to the internal Schiff base. In fact, the internal Schiff base pK_a of AspAT has been found to increase by 2 units on binding of succinate or maleate (*11*, *12*).

Like AspAT, ArAT conserves the two arginine residues in the active site (*3*, *13*; Figure 1A) and has a low internal Schiff base pK_a value of 6.6 (*1*). However, binding of the substrate analogue phenylpropionate, which has only one carboxylate, has been found to increase the pK_a value by 2.1 units, compared to the 1.6 unit increase induced by maleate (*2*). This raised a question of the validity of the electrostatic explanation (*3*) for the control of the Schiff base pK_a. Recently, we showed that the torsion angle around the C4−C4′ axis of the PLP−Lys258 Schiff base, which changes greatly during the course of catalysis, is the principal determinant of the Schiff base pK_a of AspAT (*14*). In this respect, it is important to determine whether a similar "torsion" mechanism applies to the catalytic mechanism of ArAT. Here we performed combined kinetic, spectroscopic, and mutational analyses on *E. coli* ArAT and showed that the Schiff base pK_a of this enzyme is controlled by its torsion angle rather than through electrostatic interaction.

EXPERIMENTAL PROCEDURES

Chemicals. PIPES, HEPES, and TAPS were obtained from Dojin Laboratories (Kumamoto, Japan). DL-2-Methylaspartate and DL-2-methylphenylalanine were purchased from Sigma. The medium used for bacterial growth contained 0.5% yeast extract (Nakarai Chemicals, Kyoto, Japan), 1% Polypeptone (Nihon Pharmaceuticals, Tokyo, Japan), and 0.5% NaCl at pH 7.0−7.2. All other chemicals were of the highest grade commercially available.

Preparation of the Wild-Type and Mutant Enzymes. Mutant plasmids were prepared either by using the Oligonucleotide-Directed *in vitro* Mutagenesis System version 2.1 (Amersham, Buckinghamshire, U.K.) with 22-base primers on the single-stranded pUC118-*tyrB* DNA (for R292L and R386L) or by using the Stratagene (La Jolla, CA) QuikChange Site-Directed Mutagenesis Kit with a set of complementary 40-base primers on the double-stranded pUC18-*tyrB* DNA (for K258A). The resultant mutations were CGC → CTC (R292L and R386L) and AAA → GCA (K258A). Transformation of *E. coli* cells with the wild-type and mutant plasmids and purification of the enzymes have been carried out as described previously (*15*). The PLP form of K258A ArAT was prepared according to the method of Toney and Kirsch (*16*) for K258A AspAT.

Determination of the Protein Concentration. The concentration of the ArAT subunit in solution was measured spectrophotometrically. The apparent molar extinction coefficient (ϵ_M) that was used equaled 53 000 M^{-1} cm^{-1} at 280 nm for the PLP form of the enzyme.

Spectrophotometric Analysis. Absorption spectra were measured using a Hitachi (Tokyo, Japan) U-3300 spectrophotometer. CD spectrophotometry was carried out on a JASCO (Tokyo, Japan) J-600WI spectropolarimeter. The buffer solutions for the measurements consisted of 50 mM buffer component(s) (PIPES, HEPES, or TAPS) with 0.1 M KCl and 0.1 mM EDTA. The pK_a value of the Schiff base was calculated by fitting the apparent molar absorptivity (ϵ_{app}) to eq 1, which is based on the single-ionizing group model:

$$\epsilon_{app} = (10^{-pH}\epsilon_{EH} + 10^{-pK_a}\epsilon_E)/(10^{-pH} + 10^{-pK_a}) \quad (1)$$

where ϵ_E and ϵ_{EH} represent the molar absorptivity of the basic (E_L) and acidic (E_LH^+) forms of the enzyme, respectively.

Kinetic Analysis. Stopped-flow spectrophotometry was performed using an Applied Photophysics (Leatherhead, U.K.) SX.17MV spectrophotometer. The exponential absorption changes were analyzed with the program provided with the instrument. The dead time was 2.0 ms under a pressure of 600 kPa. Time-resolved spectra were collected using the SX.17MV system equipped with a photodiode array accessory and the XScan (version 1.0) controlling software (Applied Photophysics). All the static and stopped-flow spectroscopic measurements were carried out at 298 K.

RESULTS AND DISCUSSION

Interconversion of the Two pH Forms of ArAT. The absorption spectrum of the PLP-form ArAT exhibits absorption bands at 358 nm at alkaline pH and at 430 nm at acidic pH (*1*), each representing the unprotonated and protonated forms of the internal Schiff base, respectively (*6*, *17*). The pH of the solution was rapidly changed by mixing the ArAT solution with another solution at a different pH value (pH

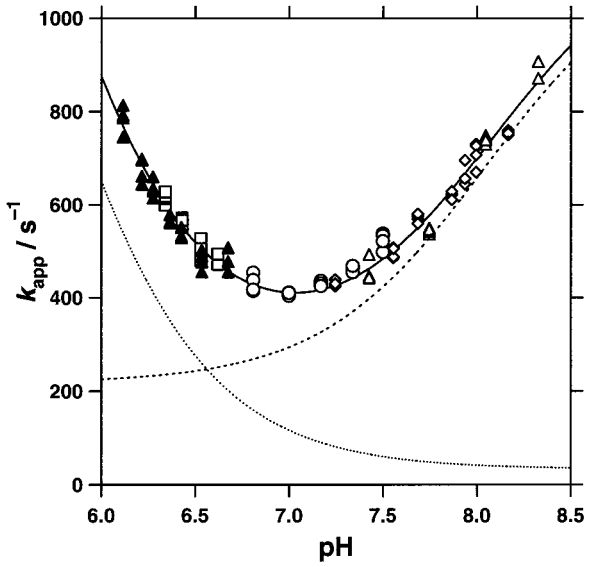

FIGURE 2: Plot of the apparent rate constant (k_{app}) for the spectral change on pH jump or drop vs the final pH of the solution. ArAT (20 μM) was mixed with various buffers at different pHs and 298 K: (○) mixed ArAT (HEPES buffer, pH 8.0) with PIPES buffer at lower pH, (□) mixed ArAT (HEPES buffer, pH 7.0) with PIPES buffer at lower pH, (▲) mixed ArAT (PIPES buffer, pH 5.7) with HEPES buffer at higher pH, (△) mixed ArAT (HEPES buffer, pH 7.0) with TAPS buffer at higher pH, and (◇) mixed ArAT (TAPS buffer, pH 9.0) with PIPES buffer at lower pH. The plot was fit according to method described previously (*18*). The values of k_E and k_{EH} are represented by the dotted and dashed lines, respectively.

jump−drop study). In the observed time range, i.e., after the dead time (2.0 ms), the absorption spectra were found to change monoexponentially, and the apparent rate constants (k_{app}) obtained at 358 and 430 nm were essentially identical (data not shown). The k_{app} value was dependent on the final pH value but was independent of the initial pH value of the enzyme solution (Figure 2). Therefore, the interconversion of the two ionic forms, the form with the internal Schiff base unprotonated (E_L) and the form with the internal Schiff base protonated (E_LH^+), could be analyzed on the basis of the following equations (*18*):[2]

$$E_L + H_3{}^+O \underset{}{\overset{K_1}{\rightleftharpoons}} E_L{\cdot}H_3{}^+O \underset{k_2}{\overset{k_1}{\rightleftharpoons}} E_LH^+ + H_2O \qquad (2)$$

$$E_L + H_2O \underset{k_4}{\overset{k_3}{\rightleftharpoons}} E_LH^+{\cdot}OH^- \underset{}{\overset{K_4}{\rightleftharpoons}} E_LH^+ + OH^- \qquad (3)$$

The apparent rate constant for the spectral change on pH jump or drop is expressed as (*18*)

$$k_{app} = k_E + k_{EH} \qquad (4)$$

where

$$k_E = k_1\frac{10^{-pH}}{K_1 + 10^{-pH}} + k_3[H_2O] = k_1\frac{10^{-pH}}{K_1 + 10^{-pH}} + k_4\frac{10^{pK_a-14}}{K_4}$$

$$k_{EH} = k_2[H_2O] + k_4\frac{10^{pH-14}}{K_4 + 10^{pH-14}} = k_1\frac{10^{-pK_a}}{K_1} + k_4\frac{10^{pH-14}}{K_4 + 10^{pH-14}}$$

Here k_E and k_{EH} are the apparent rate constants for the conversion from E_L to E_LH^+ and from E_LH^+ to E_L, respectively, and pK_a is that of the Schiff base. Fitting the data with eq 4 when pK_a = 6.6 (*1*) yielded the following values: $k_1 = 2100 \pm 400$ s^{-1}, $K_1 = (2.5 \pm 0.4) \times 10^{-6}$ M, $k_4 = 930 \pm 40$ s^{-1}, and $K_4 = (1.1 \pm 0.1) \times 10^{-6}$ M. The k_E and k_{EH} values were calculated using the above parameters and eq 4, and are shown in Figure 2. These values were used in the transient-kinetic analysis of the reaction of ArAT with substrates as described below.

Comparison of the result with that of AspAT (*18*) showed that ArAT exchanges a proton between the internal Schiff base and the solvent about 4 times faster than AspAT. Although it is hard to relate this to the functional differences between the two enzymes, the fact that ArAT has relatively large k_E and k_{EH} values should be kept in mind when we construct models for the transient kinetics of ArAT with aspartate and phenylalanine, as shown below.

Reaction of ArAT with Aspartate and Phenylalanine. To probe the comparative reactivity of E_L and E_LH^+, the change in the spectrum of ArAT on the reaction with its amino acid substrate aspartate or phenylalanine was followed at pH 6.5, where E_L and E_LH^+ exist in nearly equal amounts (Figure 3). The intensities of both the 358 and 430 nm absorption bands decreased, and a new absorption band appeared at 330 nm, indicating the formation of the pyridoxamine 5′-phosphate (PMP) form of the enzyme (E_M). In the case of the reaction with aspartate, the intensities of the absorption bands at 358 and 430 nm decreased concomitantly (Figure 3A). The concentration dependency of the apparent rate constant obtained at 430 nm was essentially identical to that at 358 nm (Figure 4A). This is in clear contrast to the case of the reaction of AspAT with aspartate, where the 358 nm absorption band disappeared rapidly, followed by a slow disappearance of the 430 nm absorption band (*18*). In the case of AspAT, within the time scale of the conversion from E_L to E_M, only a small part of E_LH^+ undergoes deprotonation to yield E_L, because the rate of interconversion between E_L and E_LH^+ of AspAT is low (k_{EH} = 88 s^{-1} at pH 7.0; *18*) compared to the rate of conversion from E_L to E_M ($k_{cat,Asp}^{half}$ = 550 s^{-1}; *19*). Therefore, in AspAT, the conversion of E_LH^+ to E_M is governed by the slow conversion of E_LH^+ to E_L. On the other hand, ArAT has a relatively small $k_{cat,Asp}^{half}$ value of 290 s^{-1} for aspartate (*1*), whereas its two ionic forms (E_L and E_LH^+) interconvert with each other fairly rapidly (see above). If this interpretation is correct, the apparent rate

[2] A more simplified mechanism that assumes direct association of $H_3{}^+O$ and OH^- with the Schiff base is expressed by the following equations: $E_L + H_3{}^+O \rightleftarrows E_LH^+ + H_2O$ ($k_1{}^\circ$ for the forward reaction and k_2 for the backward) and $E_L + H_2O \rightleftarrows E_LH^+ + OH^-$ (k_3 for the forward reaction and $k_4{}^\circ$ for the backward). This is the extreme case of eqs 2 and 3 in which k_1, K_1, k_4, and K_4 have infinite values. Equation 4 is then simplified to $k_{app} = k_1{}^\circ 10^{-pH} + k_4{}^\circ 10^{pH-14} + k_1{}^\circ 10^{-pK_a} + k_4{}^\circ 10^{pK_a-14}$. However, fitting the experimental data of Figure 2 with this equation was not satisfactory; k_{app} did not increase exponentially with increasing or decreasing pH and exhibited a tendency of saturation, which could be fit with eq 4. This may reflect indirect association of the Schiff base with the solvent H^+ and OH^-. However, the structures for $E_L{\cdot}H_3{}^+O$ and $E_LH^+{\cdot}OH^-$ are yet to be clarified. A similar result has been obtained for the protonation and/or deprotonation of the Schiff base of AspAT (*18*).

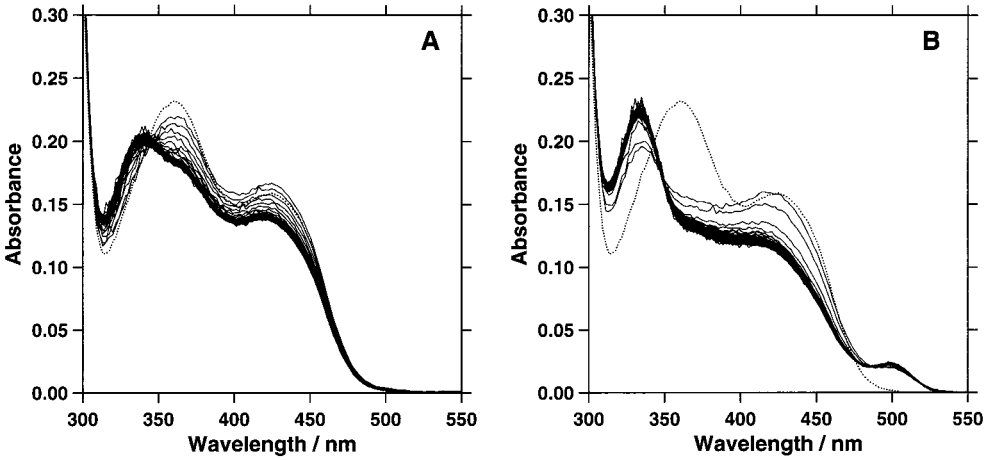

FIGURE 3: Time-dependent spectral changes of ArAT on reaction with aspartate (A) and phenylalanine (B). ArAT (46 μM) was reacted with 2 mM aspartate or phenylalanine in PIPES buffer (pH 7.0), and the spectral change was monitored using the SX.17MV stopped-flow spectrophotometer at 298 K. The spectra were taken at 2.0 ms (flow stop), 3.84 ms, and every 2.56 ms up to 254.72 ms. The initial spectrum is shown as dotted lines (A and B).

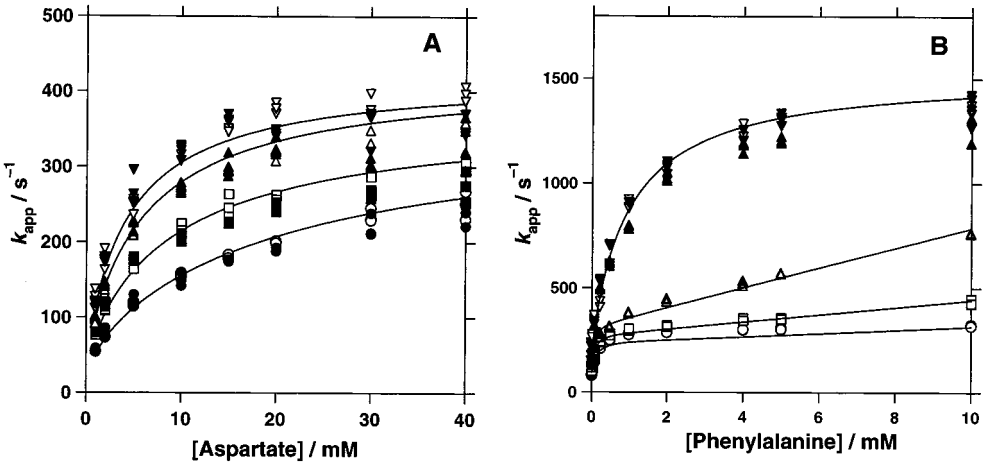

FIGURE 4: Dependency of the apparent rate constant for the change in absorption of ArAT on the substrate concentration and pH. ArAT (20 μM) was reacted with aspartate (A) or phenylalanine (B) in different pH buffer systems (PIPES/NaOH, HEPES/NaOH, and TAPS/NaOH) at 298 K: (circles) pH 6.0, (squares) pH 6.5, (triangles) pH 7.0, and (inverted triangles) pH 8.0. White and black symbols represent the values obtained at 430 and 358 nm, respectively. For the reaction with phenylalanine, the k_{app} values at 358 nm could not be obtained at pH 6.0 because of the small amplitude of the absorption change compared to the fast reaction rate.

constant should be expressed by the following equation:

$$k_{app} = \frac{[SH^+]}{(1 + 10^{pK_a^{Schiff} - pH})(K_m^{half,Asp})_{alkaline} + [SH^+]} k_{cat}^{half,Asp} + \frac{2[\overline{OA}]}{K_m^{half,OA} + 2[\overline{OA}]} k_{cat}^{half,OA} \quad (5)$$

where $(K_m^{half,Asp})_{alkaline}$ is the alkaline limiting value of the half-reaction K_m value for aspartate, $[\overline{OA}]$ is the equilibrium concentration of oxalacetate, and $[SH^+]$ is the concentration of the substrate amino acid with a protonated α-amino group. This equation is the same as the equation used for the analysis of the reaction of AspAT at high pH (*19*), except for the half-reaction K_m being multiplied by a factor of $1 + 10^{pK_a^{Schiff} - pH}$ by taking into account the fact that E_L-SH^+ is the productive combination of the enzyme−substrate ionic species at neutral pH (*20*). The theoretical lines drawn using eq 5 and the parameters, for which the values are already known (*1*), fit excellently at all pH values examined (Figure 4A). This validates the interpretation described above of the spectral behavior of ArAT in the reaction with aspartate.

The reaction of ArAT with phenylalanine exhibited a behavior similar to that of the reaction of AspAT with aspartate. Thus, the intensity of the 358 nm absorption band decreased rapidly, followed by a decrease in the intensity of the 430 nm absorption band (Figure 3B). The k_{app} value for the decrease in the intensity of the 358 nm absorption band was essentially independent of pH and was larger than the k_{app} value obtained at 430 nm (Figure 4B). Apparently, this is due to the larger k_{cat}^{half} value (1200 s^{-1}) of ArAT for phenylalanine, compared to the $E_L-E_LH^+$ interconversion rate of the enzyme.

The different behavior of the two ionic species of AspAT in the reaction with aspartate had led to the discovery of the dual substrate association process of AspAT with aspartate (*14*). Therefore, the observation with the reaction of ArAT with phenylalanine has tempted us to analyze further the reaction to examine whether a similar mechanism for the

enzyme−substrate association works in the catalytic reaction of ArAT. Considering the similarity to the reaction of AspAT with aspartate, we can draw eq 6 for the reaction of ArAT with phenylalanine:

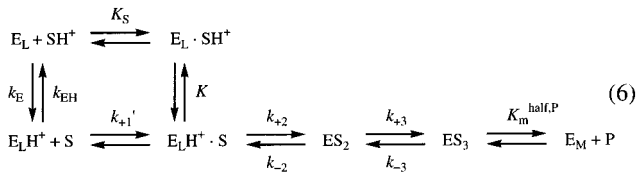

(6)

S is the substrate amino acid with the unprotonated α-amino group. The experiments were carried out at pH <8.0, where the majority of the substrate is in the SH^+ form. Therefore, we can assume a rapid equilibrium between $E_L + SH^+$, $E_L \cdot SH^+$, $E_LH^+ \cdot S$, and ES_2. Accordingly, the reaction starting from the PLP form of ArAT to the PMP form can be reduced to a two-step mechanism. The differential equations derived from this are easily solved to give the apparent rate constant as follows (*18*):

$$k_{app} = \left\{ k_{EH} + k_{+1}'[S] + Xk_E + \frac{10^{-pK_a^{\alpha}}}{10^{-pK_a^{Schiff}}} Xk_{+1}'[SH^+] + \alpha(1-X)k_{+3} + Yk_{-3} - \left[\left(-k_{EH} - k_{+1}'[S] - Xk_E - \frac{10^{-pK_a^{\alpha}}}{10^{-pK_a^{Schiff}}} Xk_{+1}'[SH^+] + \alpha(1-X)k_{+3} + Yk_{-3} \right)^2 + 4\left(Xk_E + \frac{10^{-pK_a^{\alpha}}}{10^{-pK_a^{Schiff}}} Xk_{+1}'[SH^+] \right) \alpha(1-X)k_{+3} \right]^{1/2} \right\} /2 \quad (7)$$

$$X = \frac{(K_m^{half,Phe})_{alkaline}}{(K_m^{half,Phe})_{alkaline} + [SH^+]}$$

$$Y = \frac{2[\overline{\Phi Prv}]}{K_m^{half,\Phi Prv} + 2[\overline{\Phi Prv}]}$$

$$\alpha = \frac{K_{eq}^{Phe-\Phi Prv}(K_m^{half,Phe})_{alkaline}}{K_m^{half,\Phi Prv}} \frac{k_{-3}}{k_{+3}}$$

where $(K_m^{half,Phe})_{alkaline}$ is the alkaline limiting value of the half-reaction K_m value for phenylalanine and is expressed by the following equation:

$$(K_m^{half,Phe})_{alkaline} = K_S \frac{1}{1 + \left(1 + \frac{k_{+2}}{k_{-2}}\right)K} \quad (8)$$

where $[\overline{\Phi Prv}]$ is the equilibrium concentration of phenylpyruvate. $K_{eq}^{Phe-\Phi Prv}$ is the equilibrium constant for the half-reaction and is related to the kinetic parameters in eq 6:

$$K_{eq}^{Phe-\Phi Prv} = K_S K \frac{k_{+2}}{k_{-2}} \frac{k_{+3}}{k_{-3}} K_m^{half,\Phi Prv} \quad (9)$$

We already know the values of the following kinetic parameters (*1*): $K_{eq}^{Phe-\Phi Prv} = 0.0625$, $(K_m^{half,Phe})_{alkaline} = 5.0$ mM, $K_m^{half,\Phi Prv} = 0.025$ mM, $\alpha k_{+3} = 1200\ s^{-1}$, and $k_{-3} = 490\ s^{-1}$. The values of k_E and k_{EH} can be determined from Figure 2 and eq 4 to be 650 and 230 s^{-1} (pH 6.0), 280 and 240 s^{-1} (pH 6.5), 120 and 290 s^{-1} (pH 7.0), and 42 and 660 s^{-1} (pH 8.0), respectively. Therefore, theoretical lines were drawn using eq 7, with only k_{+1}' as the adjustable parameter. The lines fit excellently to the data with the k_{+1}' value of $1.2 \times 10^7\ s^{-1}$. This supports the validity of eq 6, in which the enzyme−substrate association proceeds via dual routes, i.e., the association of the anionic form of phenylalanine and E_LH^+ and that of the zwitterionic form of phenylalanine and E_L. Thus, the substrate binding process of ArAT with phenylalanine is essentially identical to that of AspAT with aspartate.

Reactions of ArAT with 2-Methylaspartate and 2-Methylphenylalanine. We next proceeded to the analysis of the transaldimination process. For this purpose, we used 2-methylaspartate (MeAsp) and 2-methylphenylalanine (MePhe), which have no hydrogen at Cα and stop the catalytic reaction at the step of the external Schiff base. By taking into account the dual enzyme−substrate association process as described above, we can draw eq 10 for the reaction of ArAT with MeAsp and MePhe:

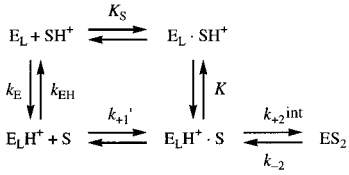

(10)

Here ES_2 is the external Schiff base complex, in which PLP forms a Schiff base with the substrate amino acid (external Schiff base) at the active site of the enzyme. At pH 8.0, the free enzyme and substrate species are essentially E_L and SH^+, respectively. Therefore, eq 10 can be reduced to eq 11, where ES_1 represents the Michaelis complex, i.e., the mixture of $E_L \cdot SH^+$ and $E_LH^+ \cdot S$.

$$E_L + SH^+ \overset{K_S/(1+K)}{\rightleftharpoons} ES_1 \underset{k_{-2}}{\overset{k_{+2}}{\rightleftharpoons}} ES_2 \quad (11)$$

There is a rapid and a small increase in the intensity of the absorption band at ∼360 nm, which occurred during the dead time. It was followed by a slow decrease in absorption intensity at 360 nm and a concomitant increase in absorption intensity at 430 nm (Figures 5A and 6A). The change in the spectrum was a monoexponential process. The apparent rate constant (k_{app}) exhibited a hyperbolic dependency on the MeAsp and MePhe concentration (data not shown) and conformed well to the following equation derived from eq 11.

$$k_{app} = \frac{[SH^+]}{K_S/(1+K) + [SH^+]} k_{+2} + k_{-2} \quad (12)$$

The following values of the parameters were determined: $K_S/(1+K) = 15 \pm 3$ mM, $k_{+2} = 440 \pm 20\ s^{-1}$, and $k_{-2} = 110 \pm 20\ s^{-1}$ for MeAsp, and $K_S/(1+K) = 8.1 \pm 0.4$ mM, $k_{+2} = 84 \pm 1\ s^{-1}$, and $k_{-2} = 82 \pm 1\ s^{-1}$ for MePhe. Using these values, we calculated the absorption spectra of ES_1 and ES_2 (Figures 5A and 6A). Using the ϵ_M value (7000

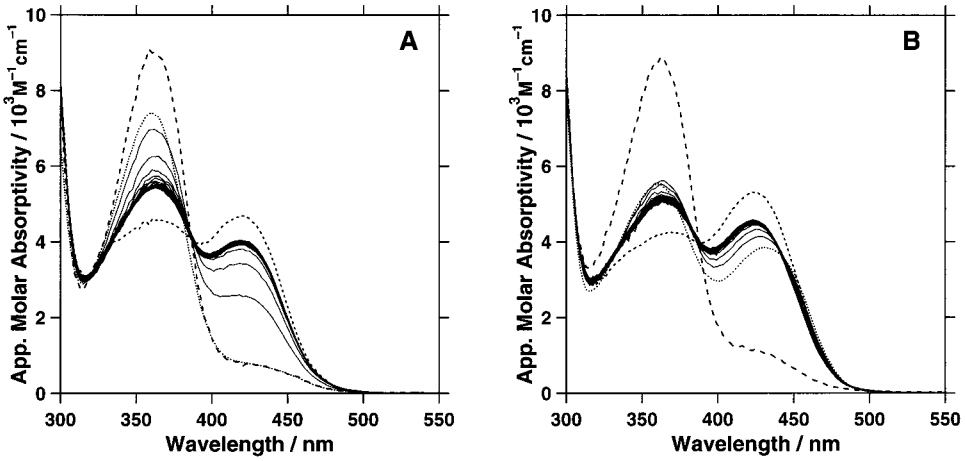

FIGURE 5: Time-dependent changes in the spectrum of ArAT on the reaction with 40 mM MeAsp at pH 8.0 (A) and pH 6.5 (B) at 298 K. Spectra were recorded in the same way as for Figure 3. Dotted lines show the initial spectrum of ArAT. Large dashed lines (with large absorption bands at 360 nm) and small dashed lines represent the spectra of ES_1 and ES_2, respectively, which were obtained from the analysis of the time-resolved spectra.

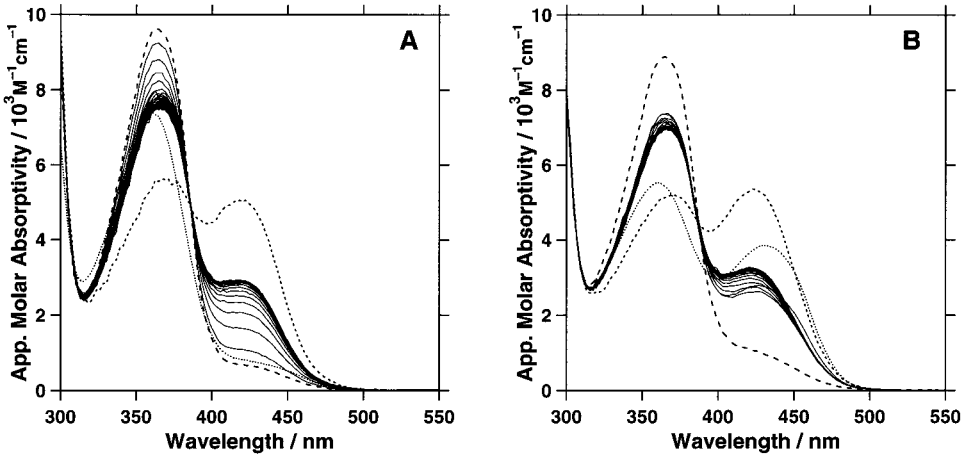

FIGURE 6: Time-dependent changes in the spectrum of ArAT on the reaction with 80 mM MePhe at pH 8.0 (A) and pH 6.5 (B) at 298 K. Experiments, analysis, and drawing of the lines were carried out in the same way as for Figure 5.

M^{-1} cm^{-1}) for E_LH^+ (*1*), we estimated that the Schiff base is 11% (MeAsp) and 9.0% (MePhe) protonated in ES_1 and 62% (MeAsp) and 65% (MePhe) protonated in ES_2. To determine whether the partial protonation of the Schiff bases in the Michaelis complex (ES_1) and the external Schiff base complex (ES_2) is affected by the solution pH, the reactions with MeAsp and MePhe were studied at pH 6.5, where E_L and E_LH^+ exist in nearly equal amounts (Figures 5B and 6B). In either case, the spectrum of ArAT exhibited a small absorption band at 430 nm and a large one at 360 nm just after the dead time. The intensity of the 430 nm band increased with the concomitant decreasing of the intensity of the 360 nm band, reaching the final spectra that resembled those at pH 8.0. This is in contrast to the observation in the reaction of AspAT with MeAsp at pH 6.8 (*14*), in which the 430 nm absorption and the 360 nm absorption bands exist with similar intensity just after the dead time, and then the 430 nm absorption intensity decreased with the concomitant increasing of the 360 nm absorption intensity. Again, we can ascribe the difference in the spectral behavior to the difference in the rate of $E_L-E_LH^+$ interconversion between ArAT and AspAT. In the case of AspAT, due to the slow conversion of E_LH^+ to E_L, the amount of E_LH^+ remains high even after E_L is converted to ES_1. Therefore, the spectrum after the dead time is that of a mixture of E_LH^+ and ES_1, each having an intense absorption band at 430 and 360 nm, respectively. In contrast, in the reactions of ArAT with MeAsp and MePhe, a large part of E_LH^+ is transformed to ES_1 via E_L, because the conversion of E_LH^+ to E_L is relatively rapid. As the result, ES_1 is the dominant species just after the dead time, and therefore, the spectrum at this time shows a large absorption at 360 nm and a small one at 430 nm (Figures 5B and 6B). With a sufficient concentration of MeAsp or MePhe, eq 10 can be reduced to eq 13 (*14*):

$$E_LH^+ \xrightarrow{k_{EH} + k_{+1}'[S]} ES_1 \underset{k_{-2}}{\overset{k_{+2}}{\rightleftharpoons}} ES_2 \qquad (13)$$

The time-resolved spectra were subjected to global analysis based on eq 13. The obtained spectra of ES_1 and ES_2 (Figures 5B and 6B) were essentially identical to those obtained at pH 8.0. The Schiff bases were 15% (MeAsp) and 13% (MePhe) protonated in ES_1 and 73% (MeAsp) and 74% (MePhe) protonated in ES_2. Therefore, in the reactions of both ArAT−MeAsp and ArAT−MePhe, the internal Schiff base in the Michaelis complex is largely unprotonated and the external Schiff base is about half-protonated, and the extents of protonation are irrespective of the solution pH. The spectra of these intermediates are essentially similar to those observed for the reaction of AspAT with MeAsp.

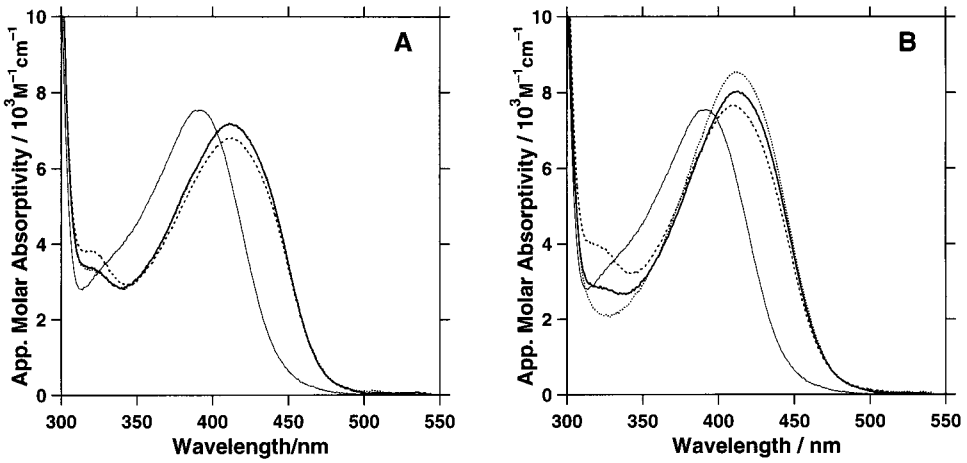

FIGURE 7: Spectra of K258A ArAT complexed with 10 mM MeAsp (A) and 10 mM MePhe (B) at 298 K: (—) pH 8.0 (50 mM HEPES/NaOH), (•••) pH 5.7 (50 mM PIPES/NaOH), and (- - -) pH 9.6 (50 mM TAPS/NaOH). The thin solid lines represent the spectra of K258A ArAT in the absence of the analogues at pH 8.0 (50 mM HEPES/NaOH). In panel A, the dotted and solid lines are almost superimposable.

To explain the pH-independent spectra of the complex of AspAT with MeAsp, a mechanism in which a proton shuttles between the imino group of the external Schiff base and the ϵ-amino group of Lys258 had been presented by Fasella and Hammes (*21*), although they postulated that the complex is entirely the external Schiff base complex (ES_2) and not the mixture with the Michaelis complex as described above. We verified this mechanism by observing the complete protonation of the PLP−MeAsp Schiff base in the K258A mutant AspAT (*14*). We applied this to our study and prepared external Schiff bases of MeAsp and MePhe with K258A ArAT (Figure 7). Due to the absence of the ϵ-amino group of Lys258 that competes with the ligand α-amino group, both of the ligands completely formed the external Schiff base. The external Schiff bases were entirely protonated even at higher pH values[3] (Figure 7), indicating that Lys258 is the base that accepts the proton from the external Schiff base. We can also apply the proton-shuttling mechanism to the Michaelis complex. In this complex, $E_L{\cdot}SH^+$ and $E_LH^+{\cdot}S$ form the proton-shuttling equilibrium and the extent of protonation is irrespective of the solution pH.[4]

Sequential Increase of the pK_a of the PLP Schiff Base. From the results described above, we can consider a scheme for the reaction of ArAT with its amino acid substrates similar to that for the reaction of AspAT with aspartate (Scheme 1). From the fraction of the protonated form of the Schiff base determined from the transient kinetics, we could estimate the following equilibrium constants: $[E_L{\cdot}SH^+]/[E_LH^+{\cdot}S] = 5.7-8.1$ (MeAsp) and 6.7−10 (MePhe), and $[H^+E_L{=}S]/[E_LH^+{=}S] = 0.37-0.61$ (MeAsp) and 0.35−0.53 (MePhe). From these values, the differences in the intrinsic pK_a values between the Schiff base and the amino groups that share a proton with the Schiff base could be calculated. Thus, in the Michaelis complex, the pK_as of the α-amino group of MeAsp and MePhe are higher than that of the internal Schiff base by 0.76−0.91 and 0.82−1.0, respectively, and in the external Schiff base, the pK_as of the PLP−MeAsp and PLP−MePhe Schiff bases are higher than that of the ϵ-amino group of Lys258 by 0.21−0.43 and 0.28−0.46, respectively. This indicates that the pK_a of the Schiff base is successively increased to the same extent by the dicarboxylic ligand and the aromatic (monocarboxylic) ligand. The complex of ArAT with maleate, a desamino analogue of aspartate, and that with phenylpropionate, a desamino analogue of phenylalanine, showed internal Schiff base pK_a values of 8.2 and 8.8, respectively (*2*). These values can be regarded as the intrinsic pK_a values of the PLP−Lys258 Schiff bases in the ArAT−MeAsp and ArAT−MePhe Michaelis complexes. Therefore, the pK_a values of the α-amino group of MeAsp, and that of MePhe, in the Michaelis complexes were estimated to be 9.0−9.1 and 9.6−9.8, respectively. For MeAsp, the value is lower than the value in the aqueous solutions by 1.5−1.6 (*14*), reflecting the decrease in basicity of the α-amino group on entering into the enzyme active site that is less polar than the solution. The pK_a values of the external Schiff bases are at ≥10.5, because the Schiff bases are almost protonated at 9.5 (Figure 6; see footnote 3). This conforms to the observation that the intrinsic pK_a of the external Schiff base is 0.2−0.5 unit higher than the pK_a (10.5 in aqueous solutions) of the ϵ-amino group of Lys258.

Electrostatic Effect of the Two Arginine Residues. The next issue is the mechanism for the increase in the Schiff base pK_a on substrate binding. First, we checked the electrostatic effect of Arg292* and Arg386 on the Schiff base pK_a. The R292L and R386L ArATs exhibited Schiff base pK_a values of 6.7 and 7.3, respectively, compared with 6.6 for the wild-

[3] In either complex, the slight decrease in the intensity of the 430 nm absorption band with increasing pH was accompanied by a concomitant increase in the intensity of the absorption band at 330 nm, and no apparent increase in the intensity of the absorption at ∼360 nm was observed. This is in contrast to the observation of the methylamine-reconstituted K258A ArAT (Figure 6), in which a small shoulder emerged at 360 nm with increasing pH, and reflects the partial deprotonation of the Schiff base. Therefore, the changes in the spectra of the complexes of K258A ArAT with MeAsp and MePhe are considered to be due to the shift in the tautomeric structure from the ketoenamine to the enolimine form of the Schiff base, although the reason for the shift is not known at present.

[4] Because the PLP Schiff base and the substrate α-amino group are considered to be close together, there would be an unfavorable electrostatic interaction if both the Schiff base and the amino group were simultaneously protonated ($E_LH^+{\cdot}SH^+$) or unprotonated ($E_L{\cdot}S$). Therefore, the structure in which the two bases share a proton, that is, the equilibrium mixture of $E_LH^+{\cdot}S$ and $E_L{\cdot}SH^+$, is the most stable (*14*). This structure, however, may not be exclusive, and the slight increase in the fraction of the protonated Schiff base with decreasing pH may reflect the emergence of the $E_LH^+{\cdot}SH^+$ structure. The same discussion applies to the external Schiff base complex, where $E_L{=}S$ and $H^+E_LH^+{=}S$ are considered unstable structures.

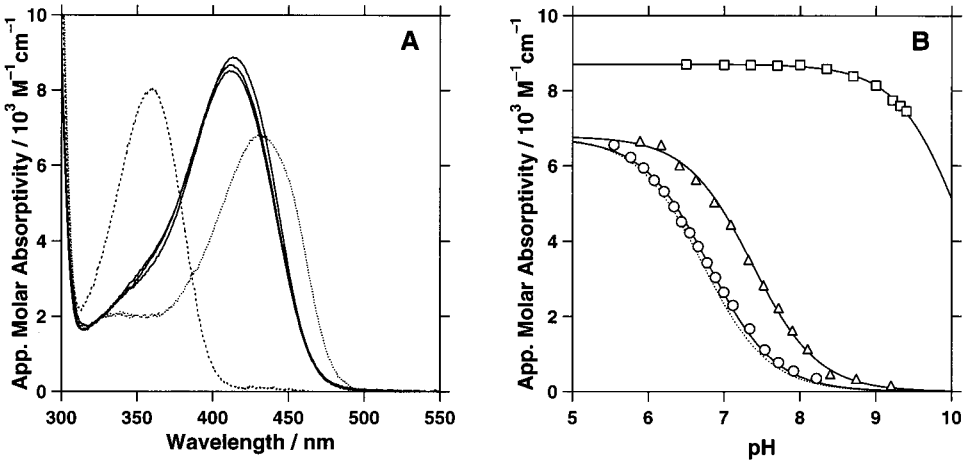

FIGURE 8: (A) Absorption spectra of K258A ArAT, in which the Schiff base was reconstituted with methylamine at 298 K. The spectra were recorded at pH 8.0, 9.0, and 9.5 (from the top to the bottom of the 413 nm absorption peak). The dotted and dashed lines represent the spectra of E_LH^+ and E_L of the wild-type enzyme, respectively. (B) pH dependence of the molar extinction coefficients of R292L (○) and R386L (△) ArATs at 430 nm and that of K258A−methylamine ArAT at 413 nm (□). Theoretical lines were drawn using eq 1. The value of ϵ_E was fixed at zero, because the unprotonated Schiff base has no absorption at >400 nm.

Scheme 1: Reaction Mechanism of ArAT with Aspartate and Phenylalanine

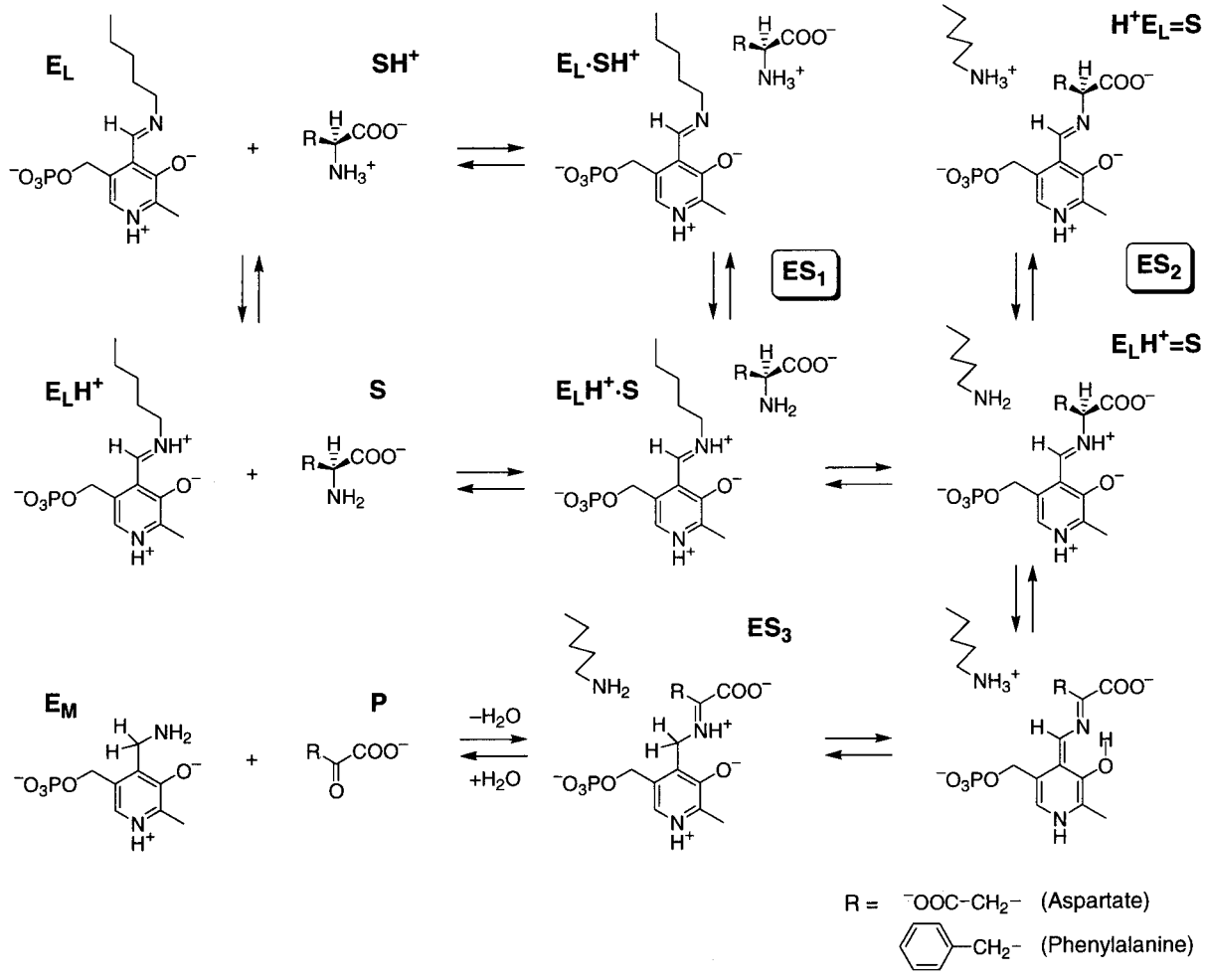

type ArAT (Figure 8B). Thus, the electrostatic effect of Arg292* on the Schiff base pK_a is almost negligible. The effect of Arg386 is larger than that of Arg292*, but it can only partially account for the increase in the Schiff base pK_a on substrate binding; the increase is 1.6 (dicarboxylic ligand) and 2.1 (aromatic ligand) in the Michaelis complex, and more than 3.9 in the external aldimines (see above). It should also be noted that the electrostatic mechanism cannot explain the difference in the Schiff base pK_a value between the Michaelis complex (ES_1) and the external aldimine (ES_2), because the electrostatic effects of the arginine residue(s) are considered to be equally masked by the carboxylate groups in the two intermediates. Therefore, we must seek other mechanisms that can control the Schiff base pK_a.

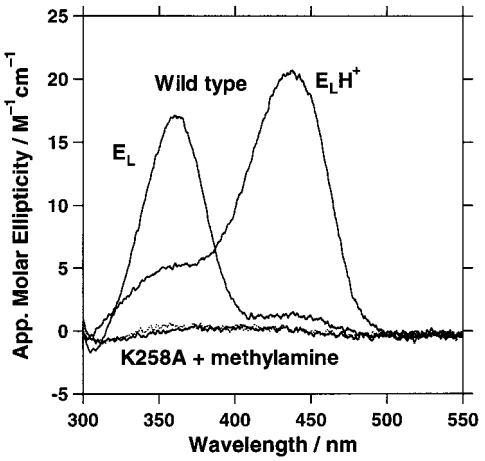

FIGURE 9: CD spectra of the wild-type and K258A−methylamine-reconstituted ArATs at 298 K. The CD spectra of the E_L and E_LH^+ forms of wild-type ArAT were determined from the values at pH 5.7 (50 mM PIPES/NaOH) and pH 8.0 (50 mM HEPES/NaOH) using the equation $\Delta\epsilon_{app} = (10^{-pH}\Delta\epsilon_{EH} + 10^{-pK_a}\Delta\epsilon_E)/(10^{-pH} + 10^{-pK_a})$. The spectra of the K258A−methylamine-reconstituted ArAT were recorded at pH 8.0 (solid line, 50 mM HEPES/NaOH) and pH 9.5 (dotted line, 50 mM TAPS/NaOH). These two lines were almost superimposable and have little CD at all the wavelengths between 300 and 550 nm.

Strain of the PLP Schiff Base. Our recent study has indicated that the torsion angle around the C4−C4′ axis of the Schiff base is the principal determinant of the PLP−Lys258 Schiff base in AspAT that can modulate its pK_a by as much as 3 units (*14*). Although the three-dimensional structure of *E. coli* ArAT with a resolution high enough to discuss the conformation of the Schiff base is not available at present (*3*), the structural similarity of ArAT and AspAT suggests that a similar mechanism works for ArAT. The K258A ArAT in which the Schiff base is reconstituted with methylamine exhibited an absorption maximum at 413 nm (Figure 8A). This absorption peak resembles that of the E_LH^+ form of the wild-type ArAT with a slight blue shift. When the pH is increased from 8.0 to 9.4, the absorbance at 413 nm slightly decreased and the absorbance at ∼360 nm concomitantly increased (Figure 8A), reflecting the partial deprotonation of the Schiff base. The exact pK_a value of this Schiff base was difficult to determine because of the elevated basicity of the Schiff base. However, if we assume that the deprotonated Schiff base has no absorption at ∼430 nm, we can roughly estimate the pK_a value to be 10.2 by fitting the data with eq 1 (Figure 8B). This indicates that the "cleavage" of the Lys258 side chain of ArAT resulted in a 3.6 pH unit increase in the pK_a of the Schiff base. The Cotton effect of >300 nm, which reflects the distortion of the PLP−Lys258 Schiff base (*14*), is nearly completely lost with the side chain cleavage (Figure 9). Therefore, we can assume that the PLP−Lys258 Schiff base of ArAT takes a distorted conformation by being tethered to the protein backbone via the side chain of Lys258, and this distortion decreases its pK_a by 3.6 units by breaking the intramolecular hydrogen bond formed between the imine N and O3′ of PLP (Figure 1B). This value is larger than that of AspAT by 0.8 unit. From this, we may expect that the PLP Schiff base in ArAT has a more strained structure than that in AspAT.

Substrate Activation Process in AspAT and ArAT. Before discussing the substrate activation mechanism of ArAT, we review here briefly the corresponding mechanism of AspAT (*14*). The pK_a of the internal Schiff base is controlled by the free energy level of the protonated Schiff base (*14*). When the substrate binds to the enzyme, the α-carboxylate group of the substrate forms hydrogen bonds with the guanidinium group of Arg386 (*22*−*24*). In addition, one of the α-carboxylate oxygens forms a hydrogen bond with Nδ of Asn194. Formation of the latter hydrogen bond would weaken the hydrogen bond between Nδ of Asn194 and O3′ of PLP, and relax partially the strain of the protonated form of the PLP−Lys258 Schiff base (*14*). Crystallographic evidence for this conjecture requires elucidation of a set of structures of the E_LH^+ form and the ligand (i.e., maleate)-bound, Schiff base-protonated form. The high-resolution structure of the maleate-bound form has been obtained for *E. coli* AspAT (1ASM; *23*) with the Nδ(Asn194)−O3′(PLP) distance being 3.02−3.31 Å (the two subunits have different values). However, the ligand-free E_LH^+ form of *E. coli* AspAT has not been obtained so far. The corresponding forms have been determined for pig cytosolic AspAT at pH 5.4 (1AJR; *4*) and chicken mitochondrial AspAT at pH 5.1 (8AAT; *24*), with the Nδ−O3′ distance being 2.97−3.02 and 2.76−3.01 Å, respectively. Thus, there is a tendency for the Nδ−O3′ distance to increase on binding of maleate. Additionally, the ligand-induced movement of the small domain toward the large domain is accompanied by the movement of the side chain of Arg386 by 1.25 Å and, concomitantly, that of Asn194 by 0.48 Å toward the Schiff base (comparison of 1ASM and 1ASN). Apparently, this contributes to relaxing the Schiff base strain. On the other hand, this obscures the increase in the Nδ−O3′ distance on binding of maleate to AspAT. In this context, we may consider that both alterations in the hydrogen-bond network and the domain movement lead to relaxation of the strain of the Schiff base. The value of the torsion angle χ (defined in Figure 1) is decreased from 30.6−42.3° (1AJR; see Figure 1) to 17.4−18.7° (1ASM). For chicken mitochondrial AspAT, the χ value is near 0°. However, in this enzyme, the C4−C4′ bond is 18° out of the plane of the pyridine ring. This will provide a strain energy similar to that of the C4−C4′ torsion, and this strain is relieved either by weakening the Nδ−O3′ hydrogen bond or by moving Asn194 toward PLP (discussed in ref *14*). The relief of the strain lowers the free energy level of the protonated internal Schiff base, and accounts for the increase in the pK_a on binding of the ligand to form the Michaelis complex (*14*).

The results of our study indicate that, for the catalytic reaction of ArAT, a ligand with only one carboxylate group can cause successive increases in the Schiff base pK_a similar to that by a ligand with two carboxylate groups. Another important finding in this study was the demonstration that, like that in AspAT, the torsion angle of C4−C4′ is likely the principal factor that decreases the pK_a in the unliganded enzyme, and its effect was estimated to be 3.6 units. Via combination of these results and with reference to the mechanism of AspAT (*14*), the reaction mechanism of ArAT with dicarboxylic and aromatic substrates can be discussed as follows. For the structural basis of the discussion, the crystal structures of a hexamutant AspAT (*25*), developed by Kirsch and Jansonius laboratories to mimic ArAT (*26*), can be used as the model for ArAT. As in the AspAT−maleate complex, the carboxylate groups of phenylpropionate and maleate bind to Arg386 and Asn194 of the hexamutant

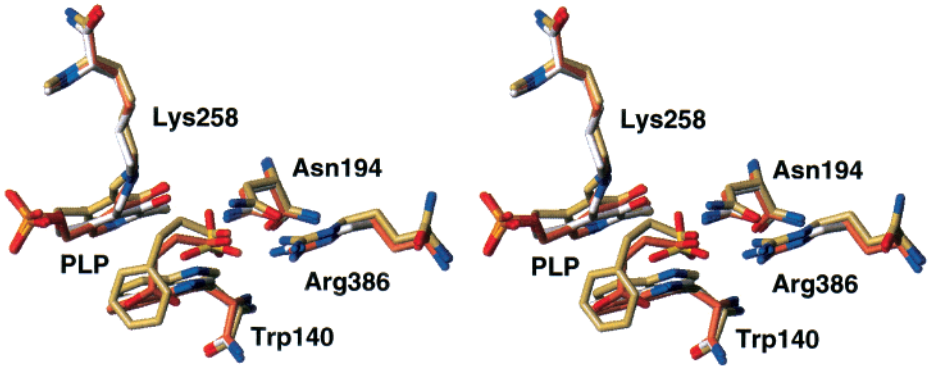

FIGURE 10: Stereodrawing of superimposed structures of the hexamutant AspAT in the sulfate-bound (1AHE), phenylpropionate-bound (1AHX), and maleate-bound (1AHY) forms. The active site of subunit A of the homodimer in the asymmetric unit is shown in each structure. The carbon atoms of 1AHX and those of 1AHY are shown in khaki and coral, respectively. The figure was drawn using MOLMOL (*27*).

ArAT (Figure 10). The torsion angle χ of the Schiff base is 28−35° in the maleate complex and 20−34° in the phenylpropionate complex. Unfortunately, the form without the analogues (1AHE) has a sulfate ion (used for crystallization) bound to Arg386 and Asn194 (Figure 10), and is not the strictly "unliganded" E_LH^+ form. However, using the data of the quantum-chemical calculation of the PLP−methylamine Schiff base (*14*), we can estimate the χ value in the E_LH^+ form of ArAT to be 40° (corresponding to 20.52 kJ mol^{-1} of the strain energy of the Schiff base calculated from the 3.6 unit increase in the pK_a of Lys258 side chain cleavage). If we assume that the Schiff base of the hexamutant AspAT has the same χ value as ArAT, we can say that the χ value is decreased by 4−12° on maleate binding and by 5−20° on phenylpropionate binding. Using the calculation data presented above, these changes in the torsion angle correspond to 0.8−1.9 unit (maleate binding) and 1.0−2.8 unit (phenylpropionate) increases in the Schiff base pK_a. These values are roughly in accordance with the observed pK_a shifts on binding of maleate (1.6 units) and phenylpropionate (2.1 units) to ArAT.

Then, what causes the relaxation of the Schiff base in ArAT (or its model enzyme, the hexamutant AspAT)? The Nδ−O3′ distance is 2.90−3.25 Å for the maleate-bound form (1AHY). The similarity of this distance of 1AHY to that of 1ASM may support the idea that the ligand binding weakens the Asn−PLP hydrogen bond and relaxes the strain. The striking structural feature of the hexamutant AspAT is that the enzyme takes the same closed conformation in the unliganded and liganded forms (*25*). Therefore, relaxation of the strain by domain movement, which has been suggested for AspAT (see above), less likely works in the hexamutant AspAT and ArAT. This may in part explain the observation (*2*) that the maleate-induced increase in the Schiff base pK_a of ArAT (1.6) is smaller than that of AspAT (2.0). In the complex of the hexamutant AspAT with phenylpropionate (1AHX), the Nδ−O3′ distance is 3.10−3.13 Å, which is similar to that of the maleate complexes of the hexamutant AspAT and AspAT, suggesting the weakened Asn−PLP hydrogen bond. Additionally, the bulky phenyl group causes reorientation of the indole ring of Trp140, and the pyridine ring of PLP, which is stacked against the indole ring of Trp140, is pushed in the direction opposite of Trp140 (upward in Figure 10). This contributes to the relaxation of the Schiff base. As the result, the χ value is further reduced in the phenylpropionate complex compared to the maleate complex. The relatively larger increase in the pK_a observed for the phenylpropionate complex (*2*) may be explained by this additional conformational effect of the phenyl ring. For the binding of aromatic ligands, the decrease in polarity of the active site on binding of aromatic ligands should also be taken into account. Generally, imines are less protonated in low-polarity environments.[5] If this is the case here, decreasing the polarity on binding of aromatic ligands cannot account for the increase in the Schiff base pK_a. In either of the bindings of dicarboxylic and aromatic ligands, the electrostatic effect of neutralization of Arg386 may contribute partially to increasing the pK_a. However, as mutation of Arg386 is expected to reduce the strain of the Schiff base by weakening the Arg386−Asn194−PLP hydrogen-bond network, the true electrostatic effect of Arg386 is likely smaller than 0.7 unit (=pK_a increment with the R386L mutation).[6] Thus, although there are some unknown factors that remain to be elucidated, we can say that the "torsion" mechanism described above can explain many of the experimental results.

The increase in the pK_a shifts the equilibrium from E_L·SH^+ to E_LH^+·S and promotes transaldimination. In the external Schiff base complex, the side chain of Lys258 that has been functioning to keep the strain of the Schiff base is liberated from PLP. The external Schiff base is fixed to a near-planar conformation, and the intramolecular hydrogen bond is stabilized (*14*). This increases further the intrinsic pK_a of the Schiff base to >10.5. The resultant increased level of protonation at the imine N enhances the electron-withdrawing ability of the conjugated system of the external Schiff base. The α-proton of the external Schiff base is then easily abstracted by the ϵ-amino group of Lys258, which is

[5] As the imine of the PLP Schiff base is in close association with the phenolic oxygen (O3′), there is a possibility that decreasing the polarity increases the Schiff base pK_a by stabilizing the protonated enolimine form relative to the protonated ketoenamine and unprotonated forms. However, the absorption spectra of the ArAT−phenylpropionate complex did not show evidence for the increase in the fraction of the enolimine form (absorbing at around 340 nm) as compared with that of the ArAT−maleate complex (*1*). In the present case, therefore, decreasing the polarity on binding of aromatic ligands is less likely the cause of the increase in the Schiff base pK_a.

[6] To dissect the two effects of the Arg386 mutation on the Schiff base pK_a, combined mutational analyses on Arg386 and the residues involved in the hydrogen-bond network, such as Asn194, are required. The analyses will be published elsewhere.

more in the unprotonated form by transferring a proton to the Schiff base. To confirm finally the hypothesis presented here, elucidation of high-resolution X-ray crystal structures of *E. coli* ArAT (or its model enzymes) both in the absence and in the presence of substrate analogues, especially those for the E_LH^+ form and the external Schiff base complex, is required.

This study also presents an important implication regarding the reaction mechanisms of the AspAT family of aminotransferases. Because most of these enzymes are active toward neutral amino acids, we encounter difficulty if we apply to these enzymes the "electrostatic" mechanism (*7*) that had been proposed for the reaction of AspAT and aspartate. The torsion mechanism does not require electrostatic effects of the substrates except for their ability to form hydrogen bonds between their α-carboxylate groups (common to all the substrate amino acids) and Arg386 and Asn194. Therefore, this mechanism is more suitable for the global understanding of the catalytic action of the AspAT family of aminotransferases.

REFERENCES

1. Hayashi, H., Inoue, K., Nagata, T., Kuramitsu, S., and Kagamiyama, H. (1993) *Biochemistry 32*, 12229−12239.
2. Iwasaki, M., Hayashi, H., and Kagamiyama, H. (1994) *J. Biochem. 115*, 156−161.
3. Ko, T.-P., Wu, S.-P., Yang, W.-Z., Tsai, H., and Yuan, H. S. (1999) *Acta Crystallogr. D55*, 1474−1477.
4. Rhee, S., Silva, M. M., Hyde, C. C., Rogers, P. H., Metzler, C. M., Metzler, D. E., and Arnone, A. (1997) *J. Biol. Chem. 272*, 17293−17302.
5. Kirsch, J. F., Eichele, G., Ford, G. C., Vincent, M. G., Jansonius, J. N., Gehring, H., and Christen, P. (1984) *J. Mol. Biol. 174*, 497−525.
6. Kallen, R. G., Korpela, T., Martell, A. E., Matsushima, Y., Metzler, C. M., Metzler, D. E., Morozov, Yu. V., Ralston, I. M., Savin, F. A., Torchinsky, Yu. M., and Ueno, H. (1985) in *Transaminases* (Christen, P., and Metzler, D. E., Eds.) pp 37−108, John Wiley and Sons, New York.
7. Ivanov, V. I., and Karpeisky, M. Y. (1969) *Adv. Enzymol. Relat. Areas Mol. Biol. 32*, 21−53.
8. Sandmeier, E., and Christen, P. (1982) *J. Biol. Chem. 257*, 6745−6750.
9. Arnone, A., Rogers, P. H., Hyde, C. C., Briley, P. D., Metzler, C. M., and Metzler, D. E. (1985) in *Transaminases* (Christen, P., and Metzler, D. E., Eds.) pp 138−154, John Wiley and Sons, New York.
10. Jansonius, J. N., Eichele, G., Ford, G. C., Picot, D., Thaller, C., and Vincent, M. (1985) in *Transaminases* (Christen, P., and Metzler, D. E., Eds.) pp 109−137, John Wiley and Sons, New York.
11. Jenkins, W. T., and D'Ari, L. (1966) *J. Biol. Chem. 241*, 5667−5674.
12. Yano, T., Mizuno, T., and Kagamiyama, H. (1993) *Biochemistry 32*, 1810−1815.
13. Kuramitsu, S., Inoue, K., Ogawa, T., Ogawa, H., and Kagamiyama, H. (1985) *Biochem. Biophys. Res. Commun. 133*, 134−139.
14. Hayashi, H., Mizuguchi, H., and Kagamiyama, H. (1998) *Biochemistry 37*, 15076−15085.
15. Inoue, Y., Kuramitsu, S., Inoue, K., Kagamiyama, H., Hiromi, K., Tanase, S., and Morino, Y. (1989) *J. Biol. Chem. 264*, 9673−9681.
16. Toney, M. D., and Kirsch, J. F. (1993) *Biochemistry 32*, 1471−1479.
17. Jenkins, W. T., and Sizer, I. W. (1957) *J. Am. Chem. Soc. 79*, 2655−2656.
18. Hayashi, H., and Kagamiyama, H. (1997) *Biochemistry 36*, 13558−13569.
19. Kuramitsu, S., Hiromi, K., Hayashi, H., Morino, Y., and Kagamiyama, H. (1990) *Biochemistry 29*, 5469−5476.
20. Kiick, D. M., and Cook, P. F. (1983) *Biochemistry 22*, 375−382.
21. Fasella, P., Giartosio, A., and Hammes, G. G. (1966) *Biochemistry 5*, 197−202.
22. Okamoto, A., Higuchi, T., Hirotsu, K., Kuramitsu, S., and Kagamiyama, H. (1994) *J. Biochem. 116*, 95−107.
23. Jäger, J., Moser, M., Sauder, U., and Jansonius, J. N. (1994) *J. Mol. Biol. 239*, 285−305.
24. McPhalen, C. A., Vincent, M. G., and Jansonius, J. N. (1992) *J. Mol. Biol. 225*, 495−517.
25. Malashkevich, V. N., Onuffer, J. J., Kirsch, J. F., and Jansonius, J. N. (1995) *Nat. Struct. Biol. 2*, 548−553.
26. Onuffer, J. J., and Kirsch, J. F. (1995) *Protein Sci. 4*, 1750−1757.
27. Koradi, R., Billeter, M., and Wüthrich, K. (1996) *J. Mol. Graphics 14*, 51−55.

BI0014709